Supplementary methods:

GSH extraction and derivatization. The procedures were modified from a previously published protocol (23). Five larval livers (including the extrahepatic biliary system) were dissected into a solution containing 100 µl of 1.25 mM 7-fluorobenz-2-oxa-1,3-diazole-4-sulfonamide (ABD-F) freshly dissolved in borate buffered saline (BBS; 0.25 mM EDTA, 25 mM $Na_2B_4O_7$) and 10 µl of 5 ng/µl [$^{13}C_2{}^{15}N_1$]-GSH as internal standard in 1% ascorbic acid. Samples were pulse sonicated, centrifuged and 10 µL of the resulting supernatant was combined with 30 µl of 5% 5-sulfosalicylic acid prior to liquid chromatography-mass spectrometry (LC/MS) analysis.

Liquid Chromatography-Mass Spectrometry (LC/MS) and Analysis. LC/MS was conducted as previously described (23) with slight modifications. Briefly, 5 µl of each sample was injected into a Waters Acquity UPLC system (Waters Corporation). Gradient separation and elution of the GSH derivative GS-ABD was performed in the linear mode employing an XBridge^{TM} C18 3.5 µm column (Waters Corporation) at a flow rate of 0.2 mL/min at room temperature. Mass spectrometry for quantitative analysis of GS-ABD was conducted on a Thermo Finnigan TSQ Quantum Ultra AM triple-stage quadrupole mass spectrometer (Thermo Finnigan) equipped with

a H-ESI source in the positive ion mode. Multiple reaction monitoring (MRM) analysis was conducted by monitoring the following selected mass transitions: m/z 505.3 → 375.9, 311.2, 182.1, m/z 508.3 → 378.9 corresponding to GS-ABD and [$^{13}C_2{}^{15}N_1$]-GS-ABD, respectively. Data were acquired and processed with the Xcalibur software application.

roGFP redox mapping. Zebrafish larvae were briefly anaesthetized with tricaine and the skin was peeled in the presence of 2 mM NEM. All samples were further incubated with NEM for 10 minutes at room temperature, and subsequently fixed with 4% paraformaldehyde for 15 minutes. Livers were then dissected and mounted in Vectashield (Vector Laboratories). The samples were allowed to equilibrate at 4°C overnight and imaged the next day on a Zeiss LSM710 laser-scanning microscope with a 20x objective. The larval livers were excited sequentially with 405 and 488 nm lasers, and the emission was detected at 500–530 nm. Images were processed by ImageJ, as previously described (25). Ratiometric images were created by dividing the 405 nm images by the 488 nm images pixel by pixel and displayed in false color with the "Fire" look-up table. Five representative areas throughout the liver were chosen per larvae to calculate the intensity of hepatocytes. The IHC were delineated by visualization of *Tp1:mCherry*.

Generation of the *Tg(Tp1:mCherry)* line. The *Tp1:mCherry* construct was generated using the multisite Gateway technology (Invitrogen) with the *p5E-Tp1*, *pME-mCherry*, and *p3E-polyA* entry clones and the *Tol2* destination vector, *pDestTol2pA2*, from the Tol2kit (44). The final construct together with *Tol2* mRNA was injected into one-cell stage embryos as previously described (44), and a stable line was established. The line is mosaic because mCherry is expressed in ~60-70% of biliary epithelial cells in the liver.

Electron microscopy of *nrf2*$^{fh318/f3h318}$ and wt sibling larvae. Transmission electron microscopy was performed by standard methods as previously described (45). Images were taken from two representative larvae from each condition.

Table S1. Multiple evolutionarily conserved stress pathways are activated in the liver of biliatresone-treated larvae. List of selected upregulated genes in the livers of biliatresone-treated (0.5 μg/ml, 4 hr) wild-type 5 dpf larvae compared to DMSO-treated controls. Livers (including EHD) from 2 clutches of biliatresone-treated and control larvae (50 livers in each clutch) were dissected and pooled for RNA extraction, library preparation followed by RNAseq. Abbreviations: UPR, unfolded protein response, ER stress, Endoplasmic reticulum stress.

Fig. S1. GSH levels are not affected by biliatresone in the larval intestine. GSH levels in the intestine and remnant larval integument after 12 hr of biliatresone treatment (bil, 0.5 μg/ml) compared with sibling control larvae. Data show mean values for three experiments with five larvae per group per experiment. Error bars, SEM.

Fig. S2. GSH depletion sensitizes intrahepatic cholangiocytes to biliatresone. Confocal projections through the livers of *Tg*(*Tp1:EGFP*) 5 dpf larvae immunostained with anti-GFP antibody. The first three images show control, biliatresone-treated (0.25 μg/ml, 12 hr), and BSO-treated (1 mM) larvae. Morphology of the IHD is normal in the control larva and larvae treated with low-dose biliatresone or BSO. In contrast, significant destruction of the IHD (*) is noted in biliatresone-treated larvae preconditioned with BSO (1 mM, 48 hr) (panel 4). Scale bar, 20 μm. Abbreviations: bil,

biliatresone; BSO, buthionine sulfoximine; IHD, intrahepatic bile ducts.

Fig. S3. Co-treatment with buthionine sulfoximine (BSO) sensitizes extrahepatic cholangiocytes to biliatresone toxicity. Confocal projections through the livers of 5 dpf wild-type control and sibling larvae treated with either biliatresone (0.25 μg/ml, 12 hr), or biliatresone and BSO. Larvae were immunostained with anti-Annexin A4 antibody. Morphology of the gallbladder (arrow) and IHD is normal in the control larva and larvae treated with low-dose biliatresone. Significant destruction of both the extrahepatic bile duct (gallbladder, arrow) and IHD (*) is noted in biliatresone-treated larvae preconditioned with BSO (1 mM, 48 hr). However, only extrahepatic cholangiocytes (gallbladder, arrow) were affected with co-incubation of biliatresone and BSO (Panel 4). Scale bar, 20 μm. Abbreviations: bil, biliatresone; BSO, buthionine sulfoximine; IHD, intrahepatic bile ducts.

Fig. S4. Histological cross sections showing normal appearance of hepatocytes in biliatresone-treated (0.50 μg/ml, 24 hr) wt and *nrf2* mutant larvae compared to controls. Abbreviations: *, gallbladder; bil, biliatresone; H, hepatocytes; *nrf2*, *nrf2*$^{fh318/fh318}$; wt, wild-type.

Fig. S5. Nrf2 inactivation leads to ER stress in hepatocytes of biliatresone-treated larvae. Transmission electron microscopy through the livers of 6 dpf wt and *nrf2* mutant larvae. Top panels show hepatocytes of wt control and sibling larvae treated with low-dose biliatresone (0.25 μg/ml, 24 hr). Bottoms panels show representative images of

identically processed *nrf2* mutant larvae. The ER appears dilated and distorted in *nrf2* larvae treated with biliatresone (arrow), suggestive of ER stress. Images are representative of two larvae per condition. Abbreviations: bil, biliatresone; C, canaliculi; *nrf2*, *nrf2*$^{fh318/fh318}$; wt, wild-type.

Fig. S6. Co-treatment with sulforaphane (SFN) does not inhibit biliatresone toxicity. Confocal projections through the livers of 6 dpf wild-type control and sibling larvae treated with either biliatresone (0.50 μg/ml, 16hr), or biliatresone and SFN. Gallbladder (arrow) injury is inhibited with SFN pretreatment (20 μM, 12 hr) but not SFN co-treatment. Scale bar, 20 μm. Abbreviations: bil, biliatresone; SFN, sulforaphane.

	Gene	Gene name	Log value
Cell redox homeostasis	*gclm*	*glutamate-cysteine ligase, modifier subunit*	2.48
	txn	*thioredoxin*	2.44
	prdx1	*peroxiredoxin 1*	2.37
	gclc	*glutamate-cysteine ligase, catalytic subunit*	1.76
	maff	*v-maf avian musculoaponeurotic fibrosarcoma oncogene homolog F*	1.98
	gsto2	*glutathione S-transferase omega 2*	1.84
	gstp1	*glutathione S-transferase pi 1*	1.33
	keap1a	*kelch-like ECH-associated protein 1a*	1.18
	dhdhl	*dihydrodiol dehydrogenase (dimeric), like*	0.9
Heat shock response	*hsp70*	*heat shock cognate 70-kd protein*	6.33
	hsp70l	*heat shock cognate 70-kd protein, like*	6.62
	hsp90aa1.2	*heat shock protein 90, alpha (cytosolic), class A member 1, tandem duplicate 2*	4.77
	hspbp1	*HSPA (heat shock 70kDa) binding protein, cytoplasmic cochaperone 1*	2.81
	hspa4a	*heat shock protein 4a*	2.02
	dnaja1	*DnaJ (Hsp40) homolog, subfamily A, member 1*	1.51
	dnajb2	*DnaJ (Hsp40) homolog, subfamily B, member 2*	1.1
UPR/ER stress	*atf3*	*activating transcription factor 3*	3.07
	nfe2l1a	*nuclear factor, erythroid 2-like 1a*	2.11
	gadd45aa	*growth arrest and DNA-damage-inducible, alpha, a*	2.01
	hspa4 (bip)	*heat shock protein 5*	1.21
	atf4b	*activating transcription factor 4b*	0.98
	ddit3	*DNA-damage-inducible transcript 3*	0.92

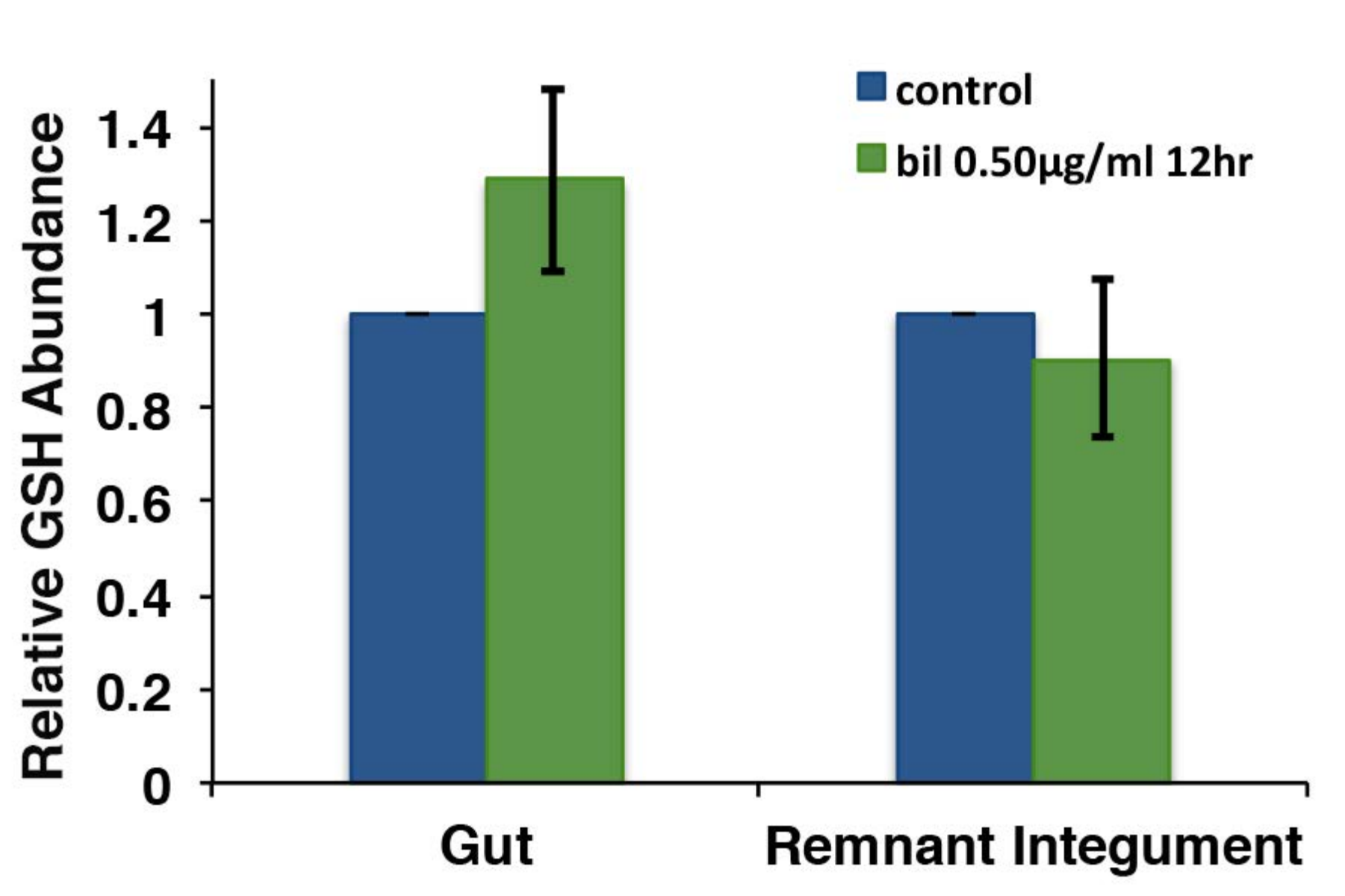
control
bil 0.50µg/ml 12hr
Relative GSH Abundance
1.4
1.2
1
0.8
0.6
0.4
0.2
0
Gut
Remnant Integument

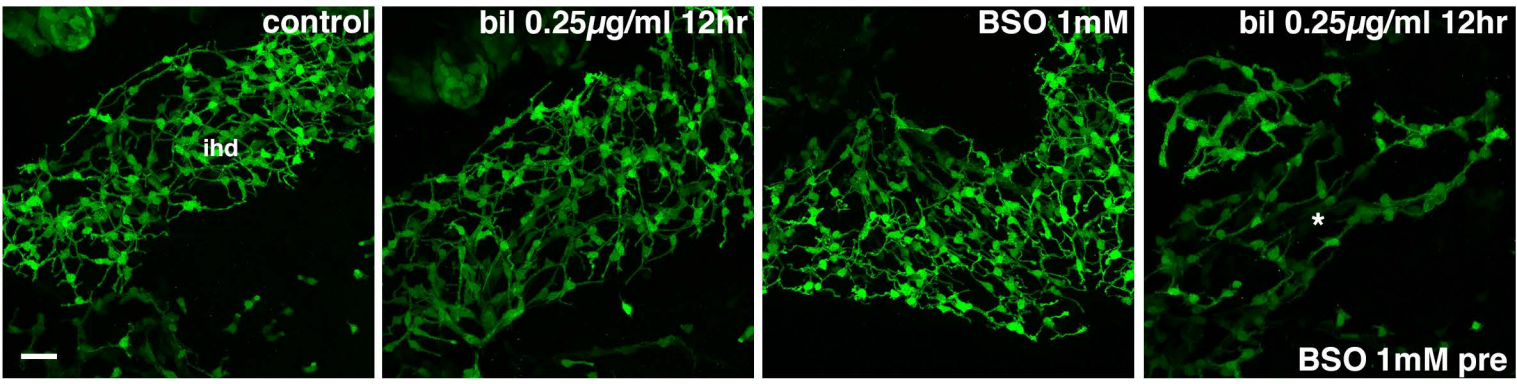
control
ihd
bil 0.25μg/ml 12hr
BSO 1mM
bil 0.25μg/ml 12hr
*
BSO 1mM pre

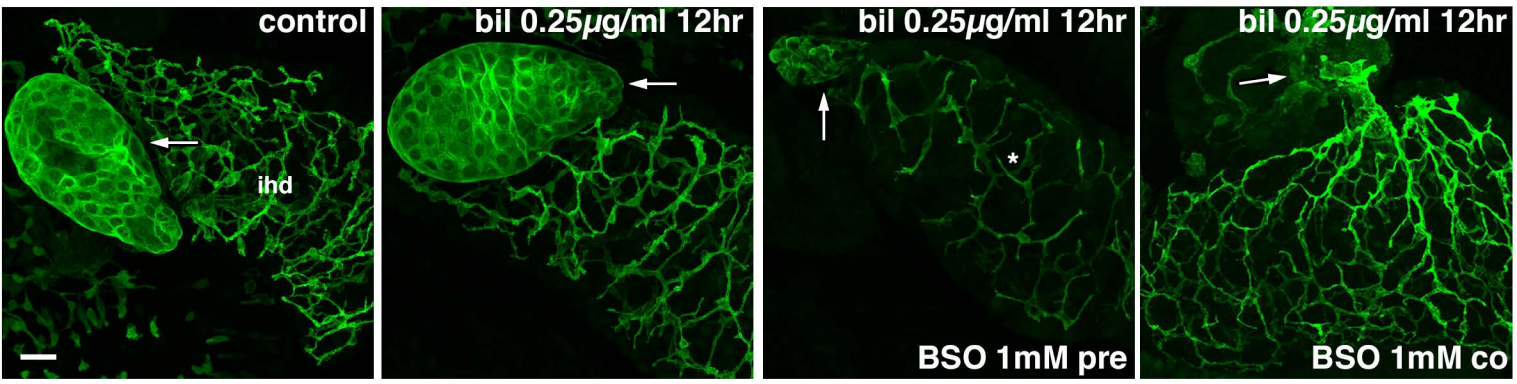
control
ihd
bil 0.25μg/ml 12hr
bil 0.25μg/ml 12hr
*
BSO 1mM pre
bil 0.25μg/ml 12hr
BSO 1mM co

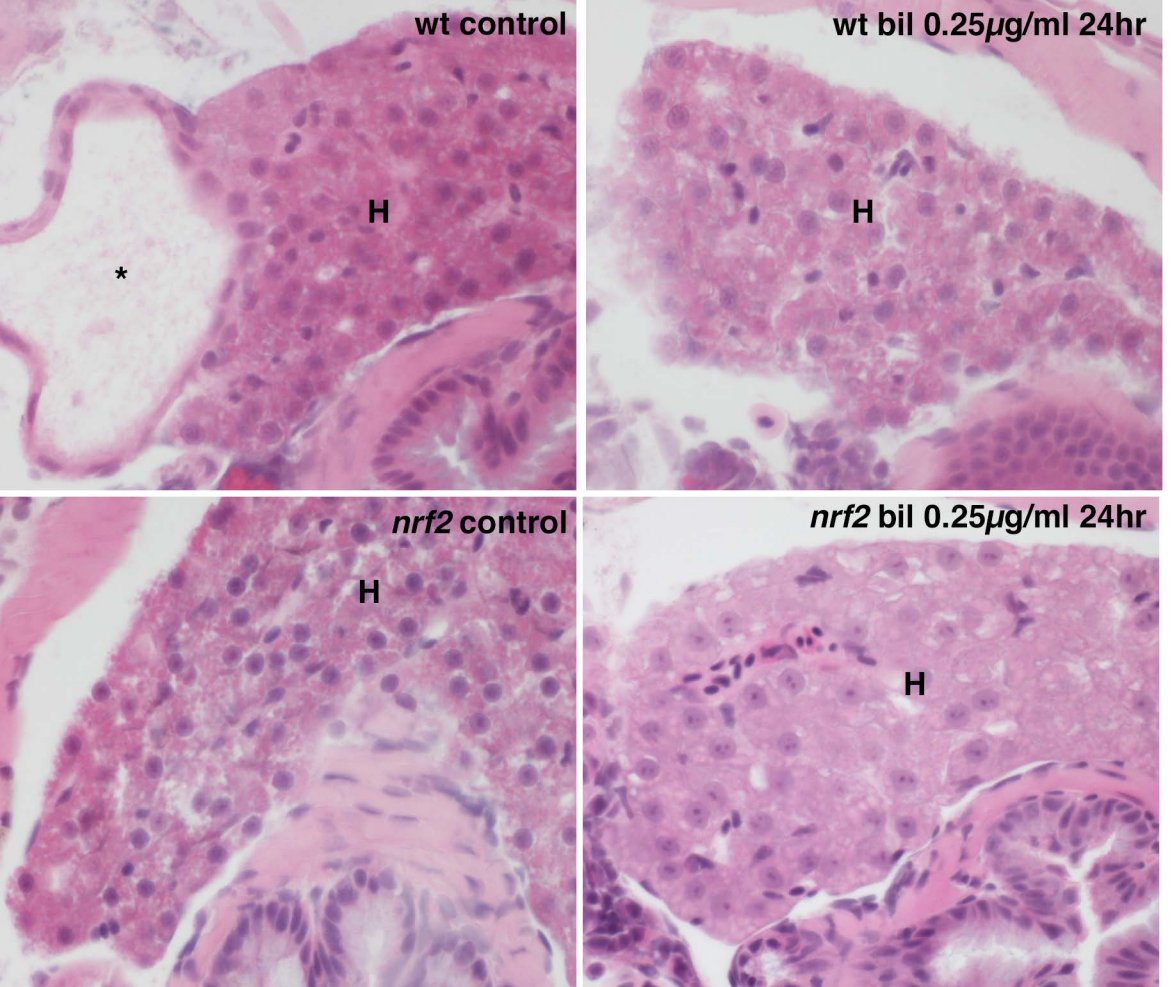
wt control
H
*
wt bil 0.25μg/ml 24hr
H
nrf2 control
H
nrf2 bil 0.25μg/ml 24hr
H

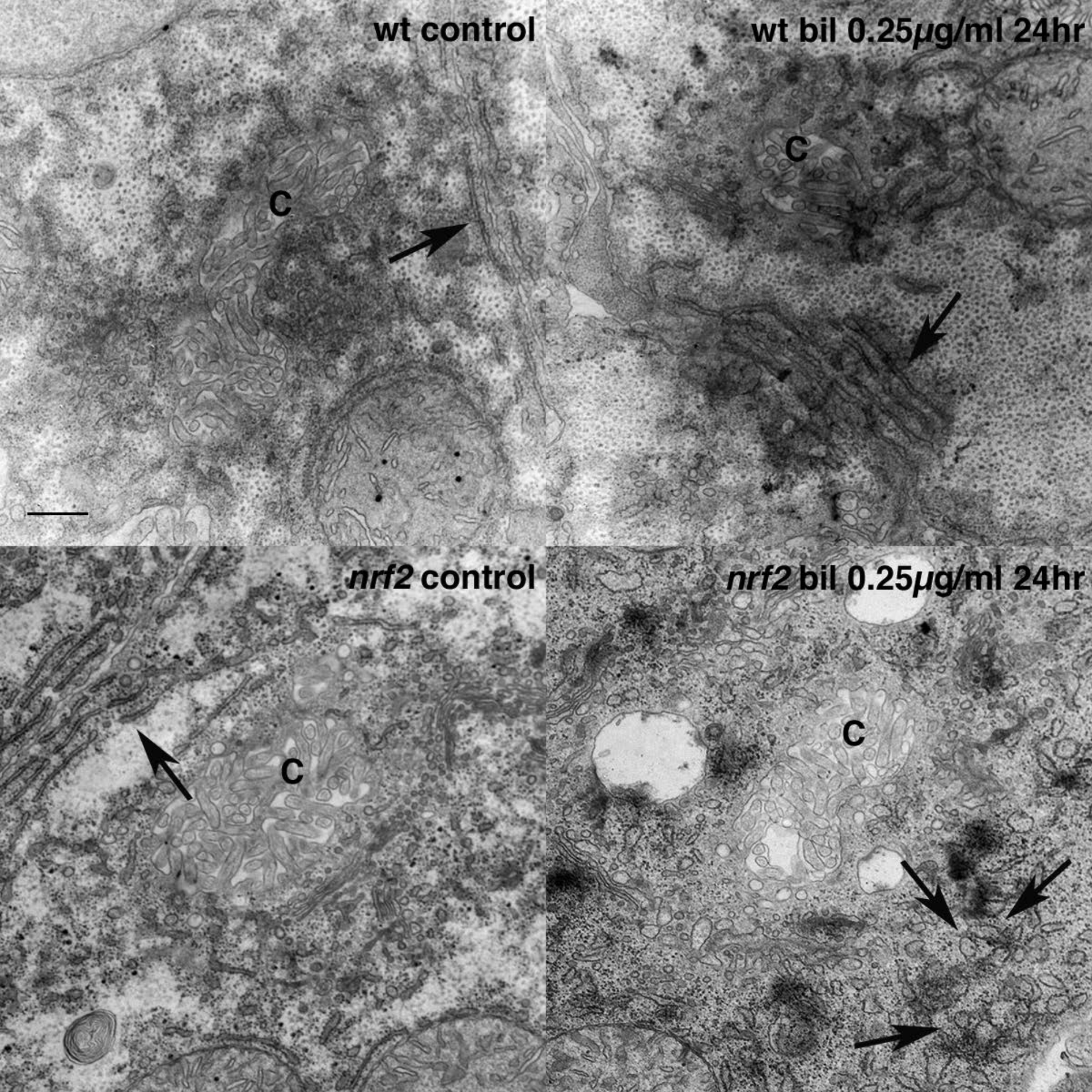
wt control
C
wt bil 0.25µg/ml 24hr
C
nrf2 control
C
nrf2 bil 0.25µg/ml 24hr
C

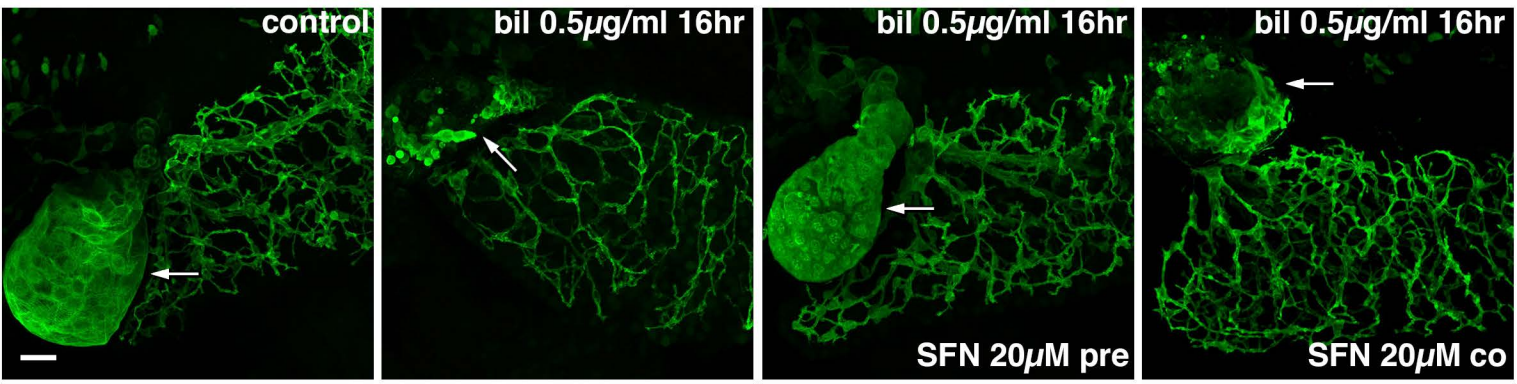
control
bil 0.5μg/ml 16hr
bil 0.5μg/ml 16hr
SFN 20μM pre
bil 0.5μg/ml 16hr
SFN 20μM co